Available online at www.sciencedirect.com
ScienceDirect
Proceedings of the Combustion Institute 31 (2007) 1543–1550
Proceedings of the Combustion Institute
www.elsevier.com/locate/proci

The effect of mixing models in PDF calculations of piloted jet flames ☆

Renfeng Richard Cao [a,*], Haifeng Wang [b], Stephen B. Pope [b]

[a] Combustion Research Facility, Sandia National Laboratories, Livermore, CA 94551, USA
[b] Sibley School of Mechanical and Aerospace Engineering, Cornell University, Ithaca, NY 14853, USA

Abstract

For turbulent flames containing significant turbulence–chemistry interactions, the accuracy of PDF model calculations depends on the accurate representation of the chemistry and on the mixing model (including the value of the mixing-model constant, C_ϕ). In recent work, Cao and Pope demonstrated that accurate calculations of the Barlow and Frank piloted jet flames D, E and F are achieved using the GRI3.0 mechanism and the EMST mixing model (with $C_\phi = 1.5$). In the present paper, further PDF model calculations (using GRI3.0) are performed in order to investigate the performance of three mixing models (EMST, IEM and MC) and their dependence on the specified value of C_ϕ. It is shown that all three models are capable of yielding levels of local extinction (quantified by a burning index) comparable to the experimental observations, but this is achieved using $C_\phi = 3.3$ for IEM, and $C_\phi = 3.8$ for MC (compared to $C_\phi = 1.5$ for EMST). However, in these calculations with IEM and MC, the mixture fraction variance is significantly underpredicted: only the EMST model is capable of calculating accurately both the observed burning indexes and the mixture fraction variance. The findings of this study, the first comparative study of mixing models in the Barlow and Frank flames, are related to previous observations.

Keywords: PDF method; Mixing model; Turbulent flame; Detailed chemistry

1. Introduction

For the computational modeling of turbulent combustion, the PDF method has the significant advantage of treating the chemical reaction source term exactly without modeling [1]. Its ability to calculate the complex non-linear interactions between turbulence and chemical reactions have been clearly demonstrated in many previous PDF calculations (e.g., [2–12]). However, in the PDF method, the effects of molecular diffusion are represented by one of several available mixing models. In previous studies, different combinations of mixing models and reaction mechanisms have been used, and our understanding of their performance remains incomplete.

The collaborative comparisons of measured and calculated results conducted within the framework of the Turbulent Non-premixed Flames (TNF) international workshop [13] greatly facilitate research work in this area. Detailed scalar and velocity measurements on the well-defined piloted methane/air jet flames reported by Barlow and coworkers [14–17] facilitate the quantitative

☆ Supplementary data for this article can be accessed online. See Appendix A.

* Corresponding author. Fax: +1 925 294 2595.
E-mail address: renfeng@gmail.com (R.R. Cao).

1540-7489/$ - see front matter © 2006 The Combustion Institute. Published by Elsevier Inc. All rights reserved.
doi:10.1016/j.proci.2006.08.052

evaluation of the chemical mechanisms and mixing models. There are many previous modeling studies of the Barlow and Frank flame D, but fewer [2,4,7,8,12] which include flame E or F, in which chemistry–turbulence interactions are more pronounced.

The recent study by Cao and Pope [12] provides a good understanding of the influence of chemical mechanisms on PDF calculations of these flames. The current work is complementary, in that the emphasis is on studying the performance of different mixing models. It has been shown that accurate calculations of flames D, E and F are obtained using the Euclidean Minimum Spanning Tree (EMST) mixing model and the GRI3.0 mechanism [18], but not if some simpler mechanisms are used. Consequently, to minimize the uncertainty in the accuracy of the chemical mechanism, in the present study we use the GRI3.0 mechanism [18], which includes 53 species and 325 reactions, and is considered to be the most comprehensive and accurate methane mechanism available at this time. Results are presented from a series of calculations of flames D, E and F using three different mixing models: The Interaction by Exchange with the Mean (IEM) model [26,27]; the modified Curl (MC) model [24,25] and the EMST model [23]. Only the EMST model is local in the composition space [23].

For the Barlow and Frank flames, this is the first comparative study of two or more mixing models, and it is also the first investigation of the performance of mixing models in combustion with the detailed GRI3.0 mechanism. Comparative studies of mixing models have previously been performed for the Delft III flame [19]; for lifted hydrogen jet flames [11]; for a counterflow flame [20]; in direct numerical simulations [21]; and in a partially stirred reactor [22]. The general observation is that (with the same value of C_ϕ) the three models can yield quantitatively different results (e.g., in scatter plots), and that the EMST model generally has a lower level of conditional fluctuations and is more resilient to extinction.

The effect of the mixing model constant C_ϕ has previously been investigated in the Barlow and Frank flames [5,7], and in other flames [3,11,19,20]. It is found that increasing the value of C_ϕ generally yields a higher conditional mean temperature and hence a more strongly burning solution. More comparison and discussion of the current and previous work will be presented later in Section 5.

In the next section, the PDF methodology used in the current work is briefly introduced. The Barlow and Frank flames and the series of calculations performed are described in Section 3. The results are presented and discussed in Section 4, and the conclusions are drawn in Section 5.

2. PDF methodology

The current work is complementary to [12] and all models and parameters used are identical to the base case described in [12]. These models and parameters are briefly listed here for reader's convenience: details can be found in [12].

The joint velocity-turbulence frequency-composition PDF method [28] is used, in which the simplified Langevin model (SLM) [29] models the evolution of the particle velocity. The stochastic frequency model of Van Slooten et al. [30] is used for the turbulence frequency of particles, which provides the time scale of turbulence. These models are the same as those used in many previous studies using the joint PDF method, e.g., [7,8,10–12,31–33]. The value of the model constants are the same as those used in [11,12,31–33]. The only difference in the constants used in earlier calculations of these flames [7,8] is that there $C_{\omega 1}$ is set to 0.56 (compared to $C_{\omega 1} = 0.65$ here). A detailed discussion and comparison of these calculations can be found in [12].

In PDF methods, the effect of molecular diffusion on the composition is represented by a mixing model. The most commonly used mixing models, and those considered here, are the EMST [23], MC [24,25] and IEM [26] (also known as LMSE [27]) mixing models. In each of these models the rate of mixing is determined by the constant C_ϕ. This is defined such that in the simplest case (of a statistically homogeneous conserved passive scalar) each model (using the same value of C_ϕ) yields the same rate of decay of scalar variance.

Radiative heat loss is accounted for using an optically thin limit radiation model [8]. The computations presented here use a code named HYB2D [11,12,31–33] which implements a hybrid finite-volume/particle algorithm. In the hybrid algorithm, the PDF/particle method (particle part) is coupled with a finite-volume solver (FV part). The FV part solves the mean conservation equations for mass, momentum, energy and the mean equation of state; and the particle part solves the modeled transport equation for the fluctuating velocity-turbulence frequency-composition PDF. The FV part provides mean fields of velocity, density and pressure to the particle part and obtains the turbulent fluxes and reaction source terms from the particle part.

The in situ adaptive tabulation (ISAT) algorithm [34] is used to implement the chemistry given by the different mechanisms. A parallel algorithm for the particle part of HYB2D, named domain partitioning of particles [11], is implemented using MPI.

The numerical parameters used for the current work are the same as those used in [12]. It has been shown in [12] that these numerical parameters ensure that the numerical errors are generally

no greater than 2% (with respect to the peak value) for the conditional mean temperature and major species, and 5% for the conditional mean minor species, at all investigated locations for flame E.

3. Calculations performed

The flames considered in this paper are the series of non-premixed piloted methane/air jet flames investigated by Barlow and Frank [14], termed flames D, E and F. These flames are statistically steady 2D axisymmetric, and non-swirling. A polar-cylindrical (z,r) coordinate system is used with the origin at the center of the fuel jet at its exit plane. The computational solution domain is rectangular, of extent $(0,80D)$ in the axial (z) direction, and $(0,20D)$ in the radial (r) direction, where D is the diameter of the jet ($D = 7.2$ mm). The boundary conditions and parameters used for the calculations are the same as the base case of [12].

Calculations have been performed of all three flames, D, E and F, although results are presented only for flame E. The value of C_ϕ is set to 1.5, 2.0, 2.5, 3.0, 3.3, 3.5, 3.8 and 4.0 for different cases. The calculated results have been extensively compared with the measurements at axial locations of $z/D = 1$, 2, 3, 7.5, 15, 30, 45, 60 and 75. The quantities investigated and compared to the measurements are velocity, mixture fraction, temperature and the mass fractions of H_2O, CO_2, N_2, O_2, CH_4, CO, H_2, OH and NO. The statistics examined include conditional and unconditional means and rms's, scatter plots and burning indexes.

4. Results

Due to the limitation of the space, only calculations of flame E, which has a significant amount of local extinction but is not too close to global extinction, are presented in this paper. The conclusions drawn based on these results have been verified with the calculations of flames D and F. The results presented are focused on the axial locations $z/D = 7.5$, 15 and 30, where most significant local extinction is observed. Unless otherwise stated, the results presented are obtained using the detailed GRI3.0 mechanism. More results can be found in the Supplementary material.

The calculations of flame E using the EMST mixing model (with all values of C_ϕ used) yield "burning solutions", i.e., flames in which essentially all the fuel is converted to products far downstream ($z/D \geqslant 60$). In contrast, with IEM a burning solution is obtained for $C_\phi = 3.3$, but there is global extinction for $C_\phi \leqslant 3.0$. Similarly, MC yields a burning solution for $C_\phi = 3.8$, but extinction for $C_\phi \leqslant 3.5$.

4.1. Calculations of the velocity field

The velocity fields display reasonable agreement (not shown, but see Section 3 of the Supplementary material) with the measurements for all "burning solutions". This includes calculations of flames D, E and F using different mixing models and/or different values of mixing model constant C_ϕ. The differences between these calculations are negligible.

4.2. Calculations of burning indexes and mixture fraction

Figure 1 compares calculations and measurements of burning indexes (BI) based on T, CO and OH as functions of axial distance. As defined previously in [7,12], BI is the ratio of the conditional mean of the quantity in a mixture fraction interval around stoichiometric to the corresponding value in a mildly strained non-premixed laminar flame. Thus, for product species, BI ≈ 1 corresponds to complete combustion and BI $= 0$ corresponds to no burning.

In the calculations shown in Fig. 1, the standard value $C_\phi = 1.5$ [7,12] is used with the EMST mixing model; whereas with IEM and MC the smallest values yielding burning solutions are used, namely $C_\phi = 3.3$ and 3.8, respectively. These values yield the closest agreement with the experimental data.

It can be seen that all three calculations generally have reasonable agreement with the measured BI(T) and BI(CO) except that the IEM calculations yield higher BI(CO) at $z/D = 7.5$ and 15. The BI(OH) obtained from calculations using IEM and MC are significantly higher than those obtained from EMST calculations and measurements.

The value of C_ϕ sensitively affects the calculations of BI, and the values used for the different models in Fig. 1 are those which yield the closest agreement with the measured BI. But most fundamentally, the value of C_ϕ affects the level of scalar fluctuations, which are examined in terms of the rms of mixture fraction (ξ'). Figure 2 shows radial profiles of the mean and rms mixture fraction (all the mean and rms mixture fraction in this paper are Favre mean) from the calculations with the three mixing models (again with $C_\phi = 1.5$ for EMST, $C_\phi = 3.3$ for IEM and $C_\phi = 3.8$ for MC).

One can see from Fig. 2 that the EMST calculations are in good agreement with the experimental data both for the mean and rms mixture fraction at all locations. On the other hand, the IEM and MC mixing models significantly underpredict the rms mixture fraction at all locations

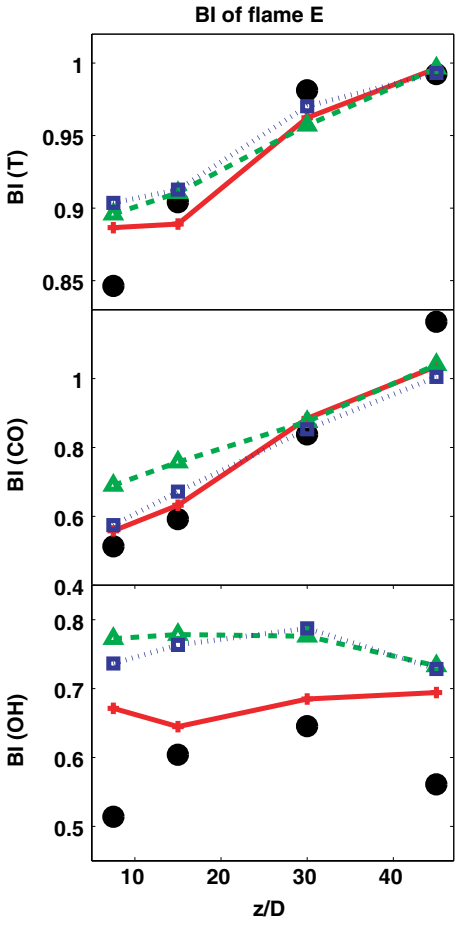

Fig. 1. Axial variation of Burning Indexes in flame E obtained using EMST, IEM and MC with different values of C_ϕ. Solid circles are the measurements and lines are joint PDF calculations: red solid with plus, EMST with $C_\phi = 1.5$; green dashed with triangle, IEM with $C_\phi = 3.3$; blue dotted with square, MC with $C_\phi = 3.8$. (For interpretation of the references to color in this figure legend, the reader is referred to the web version of this paper.)

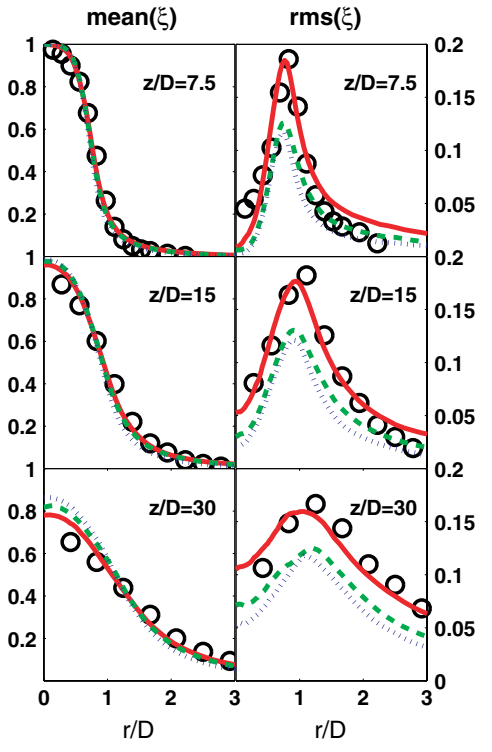

Fig. 2. Radial profiles of Favre mean and rms mixture fraction in flame E at $z/D = 7.5$, 15 and 30 obtained using EMST, IEM and MC with different values of C_ϕ. Circles are the measurement and lines are joint PDF calculations: red solid, EMST with $C_\phi = 1.5$; green dashed, IEM with $C_\phi = 3.3$; blue dotted, MC with $C_\phi = 3.8$. (For interpretation of the references to color in this figure legend, the reader is referred to the web version of this paper.)

and overpredict the centerline value of the mean mixture fraction at $z/D = 30$.

4.3. Comparison of different mixing models

4.3.1. Maximum rms of mixture fraction and C_ϕ

To study further the effects of C_ϕ, we consider $\xi'_{\max}(z)$, defined as the maximum rms mixture fraction over the radial profiles at z. Figure 3 shows $\xi'_{\max}$ plotted against C_ϕ obtained using the different mixing models. Besides calculations using the detailed GRI3.0 mechanism, also shown in Fig. 3 are calculations using the MC mixing model with a five-step mechanism reduced from GRI2.11 [35,36].

With the exception of the EMST model with $C_\phi = 1.5$, it may be seen that each model yields a monotonic, approximately linear, decrease of $\xi'_{\max}$ with increasing C_ϕ, as expected from the primary role of C_ϕ in controlling the rate of scalar dissipation. There are however secondary effects, through the mean density and scalar flux, which account for the non-monotonic behavior of EMST, and for the differences between EMST and the other models.

The values of $\xi'_{\max}$ obtained from the calculations using EMST with $C_\phi = 1.5$ agree with the measurements very well, whereas those obtained from the IEM and MC mixing models are significantly smaller than the measurements. Further decreasing C_ϕ in the IEM and MC calculations using GRI3.0 yields globally extinguished solutions. However, the behavior of MC at smaller values of C_ϕ can be investigated by using the five-step mechanism [35]. The reason is that the five-step mechanism has much shorter (13–820 times) ignition delay times than those of the

GRI3.0 mechanism, and hence it is more resilient to extinction than GRI3.0, and yields burning solutions for $C_\phi \geqslant 2.0$.

As may be seen from Fig. 3, these MC/five-step calculations show ξ'_{max} decreasing approximately linearly with increasing values of C_ϕ. Similar behavior is observed for the IEM calculations using the five-step mechanism (not shown).

4.3.2. Burning indexes and the maximum rms of mixture fraction

To illustrate the capability of different mixing models to calculate both the burning indexes and the rms mixture fraction, Fig. 4 shows the burning indexes of CO against ξ'_{max} obtained from calculations using different mixing models with different values of C_ϕ.

It is clearly shown in Fig. 4 that, with the use of the detailed GRI3.0 mechanism, although the IEM and MC calculations are capable of yielding reasonable agreement with the measured burning indexes, only the EMST calculations are capable of predicting both the burning indexes and ξ'_{max} accurately.

4.4. Scatter plots and calculations of NO

For the calculations using the three different mixing models (EMST with $C_\phi = 1.5$, IEM with $C_\phi = 3.3$, and MC with $C_\phi = 3.8$), the scatter

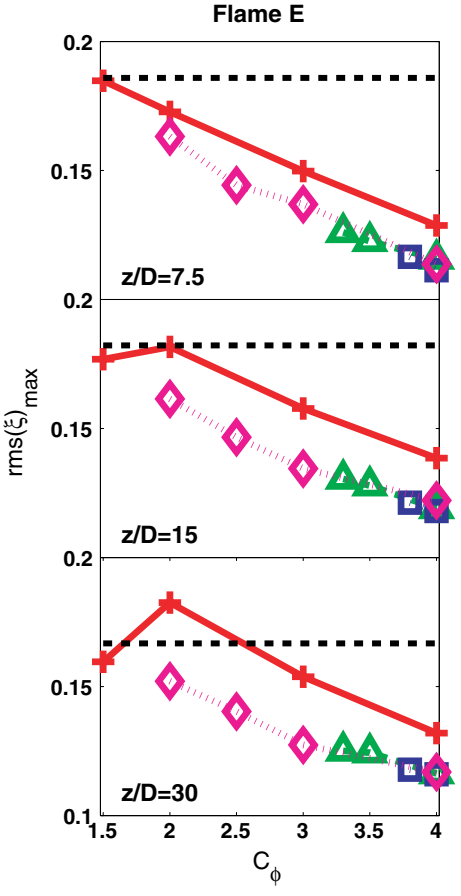

Fig. 3. Maximum rms of ξ against C_ϕ obtained using EMST, IEM and MC with the detailed GRI3.0 mechanism and the reduced five-step mechanism from GRI2.11. The horizontal dashed lines represent the experimental data and lines with symbols represent the PDF calculations. Red solid with plus, EMST with GRI3.0; green dashed with triangle: IEM with GRI3.0; blue dotted with square, MC with GRI3.0; magenta with diamond, MC with the five-step mechanism. (For interpretation of the references to color in this figure legend, the reader is referred to the web version of this paper.)

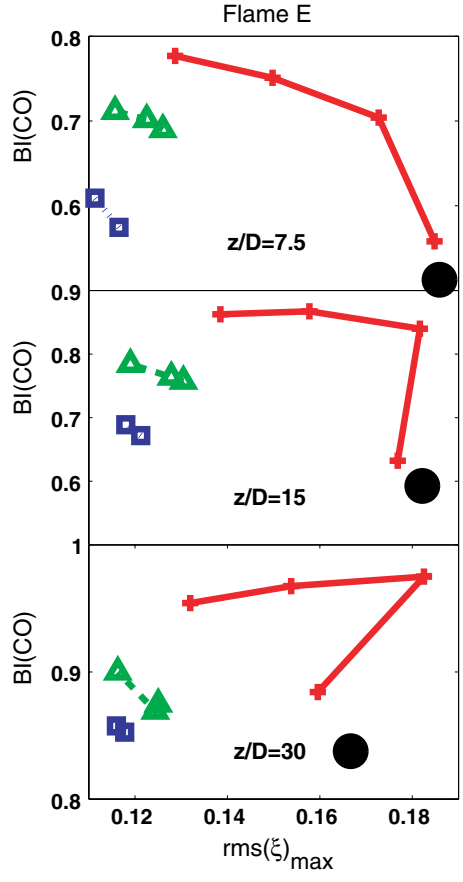

Fig. 4. Burning indexes of CO against the maximum rms of ξ obtained using EMST, IEM and MC. The solid circles represent the experimental data and lines with symbols represent the PDF calculations using different mixing models: red solid with plus, EMST; green dashed with triangle, IEM; blue dotted with square, MC. (For interpretation of the references to color in this figure legend, the reader is referred to the web version of this paper.)

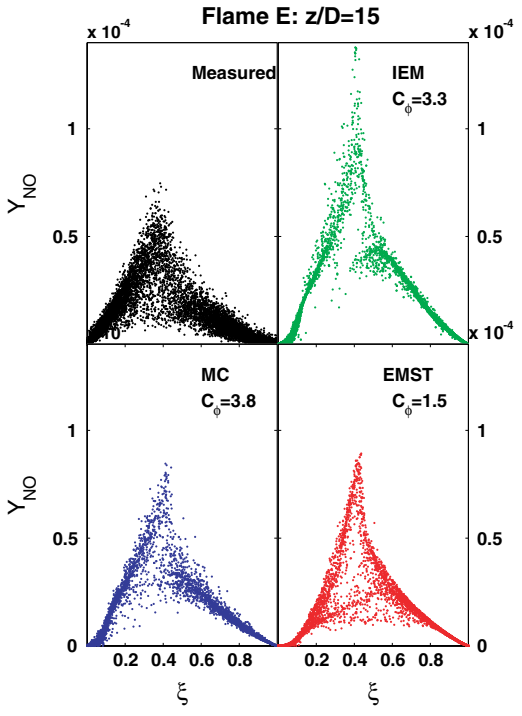

Fig. 5. Scatter plots of the mass fraction of NO obtained using different mixing models with different values of C_ϕ.

plots of temperature and species mass fractions against mixture fraction have been extensively compared (but are not shown because of space limitations, see Section 5 of the Supplementary material). There are no significant differences found between the calculations with the different mixing models. This is different than the observations in the PDF calculations of the H_2/N_2 lifted flames [11], where obvious differences are observed in the scatter plots from calculations using the three different mixing models with the same value of $C_\phi = 2.0$.

The only exception to the above is that, as shown in Fig. 5, the calculations using the IEM mixing model yield higher levels of the mass fraction of NO than those of the EMST and MC calculations (for $z/D \leqslant 30$). Although the GRI3.0 mechanism is considered to be the most comprehensive and accurate methane mechanism currently, it is known [5,12,37,38] to overpredict NO. This is also true for the current calculations as shown in Fig. 5. Nevertheless, the conclusion that IEM yields higher values of NO than do EMST and MC remains significant.

5. Discussion and Conclusions

From the present computations using the GRI3.0 mechanism, the principal observations on the relative behavior of the three mixing models are as follows:

(1) The burning index (BI) increases as C_ϕ is increased.
(2) For the EMST model, the value of $C_\phi = 1.5$ results in generally accurate calculations of both BI and the rms of mixture fraction ξ'.
(3) For IEM and MC applied to flames D and E, a larger value of C_ϕ (3.3–3.8) is required to obtain the observed levels of BI, and this leads to lower rms mixture fraction ξ' than is observed experimentally.
(4) For IEM and MC applied to flame E, a stable, burning flame is not obtained with $C_\phi \leqslant 3.0$; and for flame D and IEM a burning flame is obtained for $C_\phi = 3.0$ but not for $C_\phi = 2.0$. (These conclusions pertain to the ARM1 mechanism, whose performance has been shown [7,12] to be quite similar to GRI3.0.)
(5) When the value of C_ϕ is chosen to yield the observed levels of BI, with one exception, the conditional means given by the three mixing models are comparable (although EMST is noticeably more accurate) and the scatter plots have similar appearances.
(6) The exception to the previous conclusion is that the IEM model yields significantly higher values of NO (for $z/D \leqslant 30$).

We now relate these findings to those of previously reported PDF calculations of these and other flames. In so doing, it is important to appreciate that the calculations (the burning index in particular) depend sensitively on the chemical mechanism used, as well as on the mixing model and the value of C_ϕ.

The original calculations of Xu and Pope [7], based on the ARM1 mechanism [36] and EMST, are consistent with the above conclusions. They support, (1), (2) and (4) (in that burning solutions could not be obtained using IEM, presumably for $C_\phi \leqslant 3.0$).

The calculations of Lindstedt et al. [2] use Lindstedt's reduced mechanism and MC with $C_\phi = 2.3$. The fact that these calculations of flames D, E and F are in good agreement with the data (including BI and ξ') appears to be in conflict with (3) and (4). These findings could, however, be reconciled if the mechanism used in [2] were significantly "faster" and more resilient to extinction than GRI3.0.

Raman et al. [5] performed calculations of flame D only, using ARM1, GRI 2.11, GRI 3.0 and IEM. They obtained stable flames for $C_\phi = 2.4$, but not for smaller values—consistent with (4).

In a different methanol flame, Lindstedt and Louloudi [3] investigated the effect of increasing C_ϕ from 1.7 to 3.0 in MC and observed the same monotonic increase in BI as observed here (1).

While the present work is the first to investigate the performance of more than one mixing model in the Barlow and Frank flames, Merci et al. [19] investigated all three models (IEM, MC and EMST) in the Delft III flame using a C_1-skeletal mechanism. Their findings are generally consistent with ours: with $C_\phi = 2.0$ IEM yields extinction; MC yields a lifted flame; and only EMST correctly yields an attached flame. Increasing C_ϕ to 3.0 yields an attached flame for MC, but not for IEM. However, in distinction to (2), they find that for EMST with $C_\phi = 1.5$ the rms mixture fraction is somewhat overpredicted.

In the current work, more than 20 accurate PDF calculations with detailed GRI3.0 chemistry have been performed in a reasonably short time. This again demonstrates that this PDF/ISAT methodology can be effectively applied to turbulent flames using chemical mechanisms with of order 50 species.

Acknowledgments

This work is supported by Department of Energy under Grant DE-FG02-90ER. The computations were conducted using the resources of the Cornell Theory Center, which receives funding from Cornell University, New York State, federal agencies, foundations and corporate partners.

Appendix A. Supplementary data

Supplementary data associated with this article can be found in the online version at doi:10.1016/j.proci.2006.08.052.

References

[1] S.B. Pope, *Prog. Energy Combust. Sci.* 11 (1985) 119–192.
[2] R.P. Lindstedt, S.A. Louloudi, E.M. Váos, *Proc. Combust. Inst.* 28 (2000) 149–156.
[3] R.P. Lindstedt, S.A. Louloudi, *Proc. Combust. Inst.* 29 (2002) 2147–2154.
[4] R.P. Lindstedt, S.A. Louloudi, J.J. Driscoll, V. Sick, *Flow Turb. Combust.* 72 (2004) 407–426.
[5] V. Raman, R.O. Fox, A.D. Harvey, *Combust. Flame* 136 (2004) 327–350.
[6] H. Wang, Y. Chen, *Chem. Eng. Sci.* 59 (2004) 3477–3490.
[7] J. Xu, S.B. Pope, *Combust. Flame* 123 (2000) 281–307.
[8] Q. Tang, J. Xu, S.B. Pope, *Proc. Combust. Inst.* 28 (2000) 133–139.
[9] A.R. Masri, R. Cao, S.B. Pope, G.M. Goldin, *Combust. Theory Modell.* 8 (2004) 1–22.
[10] K. Liu, S.B. Pope, D.A. Caughey, *Combust. Flame* 141 (2005) 89–117.
[11] R.R. Cao, S.B. Pope, A.R. Masri, *Combust. Flame* 142 (2005) 438–453.
[12] R.R. Cao, S.B. Pope, *Combust. Flame* 143 (2005) 450–470.
[13] R.S. Barlow, ed., Sandia National Laboratories, available at <http://www.ca.sandia.gov/TNF/>.
[14] R.S. Barlow, J.H. Frank, *Proc. Combust. Inst.* 27 (1998) 1087–1095.
[15] J.H. Frank, R.S. Barlow, C. Lundquist, *Proc. Combust. Inst.* 28 (2000) 447–454.
[16] Ch. Schneider, A. Dreizler, J. Janicka, E.P. Hassel, *Combust. Flame* 135 (2003) 185–190.
[17] R.S. Barlow, A.N. Karpetis, *Proc. Combust. Inst.* 30 (2005) 673–680.
[18] GRI-Mech Web site, available at <http://www.me.berkeley.edu/gri-mech/>.
[19] B. Merci, D. Roekaerts, B. Naud, *Combust. Flame* 144 (2006) 476–493.
[20] J.D. Blouch, J-Y. Chen, C.K. Law, *Combust. Flame* 135 (2003) 209–225.
[21] S. Mitarai, J.J. Riley, G. Kosály, *Phys. Fluids* 17 (2005) 47101–47115.
[22] Z. Ren, S.B. Pope, *Combust. Flame* 136 (2004) 208–216.
[23] S. Subramaniam, S.B. Pope, *Combust. Flame* 115 (1998) 487–514.
[24] R.L. Curl, *AICHE J.* 9 (1963) 175–181.
[25] J. Janicka, W. Kolbe, W. Kollmann, *J. Non-Equilib. Thermodyn.* 4 (1979) 47–66.
[26] J. Villermaux, J.C. Devillon, *Proc. Second Int. Symp. On Chemical Reaction Engineering*, Elsevier, New York, 1972.
[27] C. Dopazo, E.E. O'Brien, *Acta Astronaut.* 1 (1974) 1239–1266.
[28] S.B. Pope, *Turbulent Flows*, Cambridge University Press, 2000.
[29] D.C. Haworth, S.B. Pope, *Phys. Fluids* 29 (1986) 387–405.
[30] P.R. Van Slooten, Jayesh, S.B. Pope, *Phys. Fluids* 10 (1998) 246–265.
[31] P. Jenny, M. Muradoglu, K. Liu, S.B. Pope, D.A. Caughey, *J. Comp. Phys.* 169 (2001) 1–23.
[32] M. Muradoglu, S.B. Pope, D.A. Caughey, *J. Comp. Phys.* 172 (2001) 841–878.
[33] M. Muradoglu, K. Liu, S.B. Pope, *Combust. Flame* 132 (2003) 115–137.
[34] S.B. Pope, *Combust. Theory Modell.* 1 (1997) 41–63.
[35] H.P. Mallampalli, T.H. Fletcher, J.Y. Chen, *Paper 96F-098*, presented at the Fall Meeting of the Western States Section of the Combustion Institute, University of Southern California, Los Angeles, CA October 28–29, 1996.
[36] C.J. Sung, C.K. Law, J.Y. Chen, *Proc. Combust. Inst.* 27 (1998) 295–304.
[37] H. Pitsch, H. Steiner, *Phys. Fluids* 12 (2000) 2541–2554.
[38] R.S. Barlow, A.N. Karpetis, J.H. Frank, J.Y. Chen, *Combust. Flame* 127 (2001) 2102–2118.

Comments

Bart Merci, Ghent University, Belgium. There is a non-monotonic evolution toward the experimental data of rms (ξ) as C_ϕ is decreased with the EMST mixing model. Is there an explanation for this observation? Could it be related to the fact that scalar dissipation rate is not necessarily directly proportional to C_ϕ?

Reply. We are confident that the non-monotonic behavior at $x/D = 15$ and 30 observed in Fig. 3. is a true model prediction (as opposed to numerical error). While the precise origin of this behavior has not been identified, there are several possibilities. The most likely is that as C_ϕ is increased from 1.5 to 2.0, the level of local extinction decreases and the changed mean density leads to an increase in rms (ξ).

●

Daniel C. Haworth, Pennsylvania State University, USA. The effect of mixing models has been addressed in this paper, and chemical kinetics has been addressed earlier [1]. Can you comment on the importance of the level of closure in PDF-based calculations of piloted jet flames? For example, here a velocity–composition–frequency PDF has been used, while other researchers have used a composition PDF with a Reynolds-stress turbulence closure, or a composition PDF with k–e turbulence closure.

Reference

[1] R.R. Cao, S.B. Pope, *Combust. Flame* (2005) 450–470..

Reply. We have so far focused on chemical mechanisms and mixing models because, as far as the combustion is concerned, these are the most important submodels in our velocity-frequency-composition PDF methodology. It is, however, correct to observe that another difference between our calculations ([7,8,12] in paper) and those of Lindstedt et al. ([2] in paper) is the level of PDF closure (velocity-frequency-composition compared to composition). It seems that there have been no published comparisons of the different levels of PDF closure applied to the Barlow and Frank flames using the same chemical mechanism and mixing model. This is a useful area for future research.

●

Larry Baxter, Brigham Young University, USA. During the question and answer session, you outlined an argument that the remaining discrepancies between model predictions and measurements, especially with respect to NO, arise from inadequacies in chemical kinetics as opposed to conceptual or mathematical inaccuracies in the modeling approach. Please summarize this argument again and indicate where, if at all, residual model weaknesses apparent by comparison to data may lie.

Reply. The PDF calculations of the Barlow and Frank flames using the GRI 3.0 mechanism and the EMST mixing model (with $C_\phi = 1.5$) reported here and in Cao and Pope ([12] in paper) agree well with the experimental data, except with respect to NO. The laminar flame calculations of Barlow et al. ([38] in paper) for the same fuel/air mixture and using GRI 3.0 show a similar over prediction of NO. It is for this reason that we conclude that the discrepancy between the calculated and measured NO levels in the turbulent flames is due to deficiencies in the NO chemistry in GRI 3.0.